Nucleic Acids Research, 2026, **54**, gkaf1485
https://doi.org/10.1093/nar/gkaf1485
Nucleic Acid Enzymes

Nuc domain electrostatics drive the *trans* cleavage activity of CRISPR–Cas12a

Anthony Newman*, Lora Starrs, Gaetan Burgio*

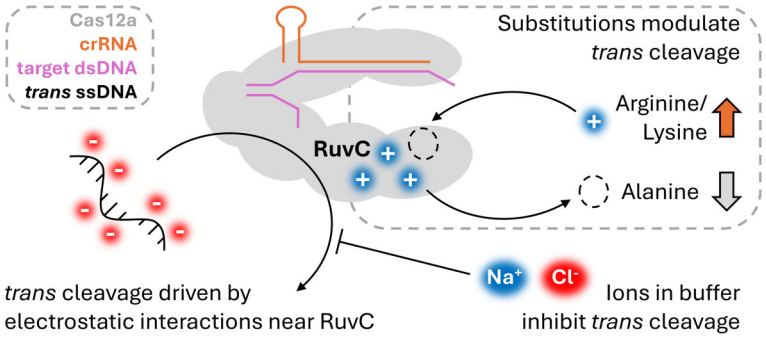
The Shine-Dalgarno Centre for RNA Innovation, Division of Genome Sciences and Cancer, The John Curtin School of Medical Research, The Australian National University, Canberra ACT 2601,Australia

*To whom correspondence should be addressed. Email:anthony.newman@anu.edu.au
Correspondence may also be addressed to Gaetan Burgio. Email: gaetan.burgio@anu.edu.au

Abstract

The *trans* cleavage activity of Cas12a has been extensively used for the detection of biomolecules. Different Cas12a orthologues exhibit faster or slower *trans* cleavage kinetics, making some orthologues more suited for sensitive molecular detection. Ionic strength of reaction buffers and mutations that change the electrostatic environment near the RuvC active site have also been reported to strongly influence *trans* cleavage kinetics. Studying three commonly used Cas12a orthologues (FnCas12a, AsCas12a, and LbCas12a), we report that electrostatic interactions near the RuvC active site are critical for their *trans* cleavage activity. Alanine substitution of arginine and lysine residues in the Nuc domain can abolish *trans* cleavage while modestly reducing *cis* cleavage. Substitutions in the RuvC lid and substitutions to introduce positively charged residues in the Nuc could enhance both *cis* and *trans* cleavage. These Cas12a variants improved DNA detection and genome editing efficacy. Overall, this study provides a blueprint for rationally engineering the DNase activities of Cas12a.

Graphical abstract



Introduction

The DNase activities of CRISPR–Cas12a (clustered regularly interspaced short palindromic repeats, CRISPR-associated) have been widely employed for sensitive molecular detection [1]. Cas12a has specific RNA-guided cleavage of dsDNA (*cis* cleavage) and remains catalytically active to non-specifically cleave ssDNA, RNA, and even nick dsDNA (*trans* cleavage) [2–5]. Thus, the presence of the programmed DNA target is signalled by *trans* cleavage of a suitable reporter molecule. Reverse transcription of RNA can generate a suitable target for *cis* cleavage, and various aptamer strategies can then activate *cis* cleavage in the presence of proteins, small molecules, and numerous other analytes [6]. *Trans* cleavage may then be detected by fluorescence, colorimetry, lateral flow strips, or electrochemical methods [1].

Cas12a binds dsDNA and initiates duplex unwinding at specific nucleotide motifs (the protospacer adjacent motif, or PAM) [5]. This allows the crRNA (CRISPR-RNA) of Cas12a to base-pair to an unwound strand of DNA, the target strand (TS) [7, 8]. Dynamic motions of the recognition (REC) lobe are stabilized through binding to a matching crRNA:TS heteroduplex, which in turn allosterically activates the RuvC active site by stabilizing the open state of the RuvC 'lid' loop [9, 10]. Then, single unwound DNA strands can be coordinated in the active site cleft for cleavage [9, 11]. The non-hybridized or non-target DNA strand (NTS) is cleaved first, being coordinated by a positively charged groove in the nuclease (NUC) lobe, close to the active site cleft, and in the required 5′ to 3′ polarity for Mg^{2+}-mediated phosphodiester bond cleavage [7–9, 11]. The scissile phosphate of the TS must twist sharply and traverse ∼20 Å between the REC and NUC lobes to access the active site; thus, rates of TS cleavage are 2–20× slower than NTS cleavage [7–9, 11–16].

Biochemical and structural evidence points to a number of key residues involved in coordinating DNA strands in the active site cleft for cleavage. A conserved arginine in the

Received: November 10, 2025. **Revised:** December 7, 2025. **Accepted:** December 11, 2025
© The Author(s) 2026. Published by Oxford University Press.
This is an Open Access article distributed under the terms of the Creative Commons Attribution License (https://creativecommons.org/licenses/by/4.0/), which permits unrestricted reuse, distribution, and reproduction in any medium, provided the original work is properly cited.

Downloaded from https://academic.oup.com/nar/article/54/1/gkaf1485/8418215 by guest on 26 March 2026

Nuc domain is adjacent to the RuvC active site residues and is thought to coordinate the scissile phosphate immediately prior to 'passing it on' to the Mg^{2+} ions [7–9, 11, 17]. A conserved phenylalanine in the RuvC lid makes base-stacking interactions with incoming substrates, effectively 'pinning' DNA strands in the active site [9, 18]. Alanine substitution of either residue is deleterious to *cis* and *trans* cleavage [7–9, 11, 17, 18]. More broadly, networks of interactions in the Nuc and Nuc-loop also aid coordination of DNA strands for *cis* cleavage [9, 11, 12].

Several studies have identified that *trans* cleavage rates are sensitive to the ionic strength of the reaction buffer [3, 19, 20]. For example, increasing NaCl concentration slows *trans* cleavage, and buffers lacking NaCl have higher *trans* cleavage rates [3, 19, 20]. Moreover, Cas12a orthologues themselves have varying rates of *trans* cleavage [2, 3, 12]. We hypothesized that key electrostatic interactions could be driving *trans* cleavage and that these vary between Cas12a orthologues.

To test this hypothesis, we performed alanine substitution of positively charged residues in the Nuc across three Cas12a orthologues (FnCas12a from *Francisella tularensis* subsp. *novicida U112*, AsCas12a from *Acidaminococcus* sp. *BV3L6*, and LbCas12a from *Lachnospiraceae bacterium ND2006*). We found that alanine substitution could abolish *trans* cleavage while retaining *cis* cleavage. This complements literature observations of ionic strength of reaction buffers decreasing *trans* cleavage rates by neutralizing non-specific electrostatic protein–nucleic acid interactions [19]. To engineer Cas12a nucleases with higher *cis* and *trans* cleavage, we assessed mutations in the RuvC-lid and performed substitutions to introduce more positively charged residues in the Nuc domain. These variants exhibited higher *trans* cleavage, especially at higher NaCl concentrations, enhancing their DNA detection ability. Engineered variants also have increased *cis* cleavage kinetics and improved genome editing activity.

Materials and methods

Structural analyses

Structural data of Cas12a orthologues were accessed from PDB (rcsb.org) or EMBL/AlphaFold databases (6GTG and 6I1K—FnCas12a, 8SFR—AsCas12a, A0A182DWE3—LbCas12a) [21]. Structures were visualized in ChimeraX (version 1.9) [22].

Cloning, protein purification, and protein thermostability

Site-directed mutagenesis was used to generate point mutants of Cas12a orthologues. Template plasmids were pET21a-Cas12a-3×HA-2×NLS constructs, as used previously [12]. Q5 site-directed mutagenesis was performed as per the manufacturer's instructions (NEB), using primers in Supplementary Table S1. Sequences were verified by Sanger sequencing (performed at the Biomolecular Resource Facility, ANU). Cas12a proteins were obtained by overexpression and purification from T7Express cells (NEB), as previously described, with no modifications [12]. Likewise, protein thermostability assays were performed precisely as previously described [12].

Trans cleavage kinetics

Assays for *trans* cleavage kinetics were performed by assembling a Cas12a–crRNA complex, followed by incubation with target DNA to allow the *cis* cleavage reaction to go to completion. Then, excess reporter ssDNA was added to achieve pseudo-first-order reaction conditions.

Oligonucleotides for crRNA and DNA targets (Supplementary Table S2) were purchased from Integrated DNA Technologies (IDT) and resuspended in 1× IDTE buffer (IDT). Double-stranded DNA targets were made by annealing 10 μM each of TS and NTS oligos in 1× Duplex Buffer (IDT), heating to 90°C in a thermocycler, and cooling at 1°C per 30 s until 20°C. DNA targets for *cis* cleavage (1 nM, unless otherwise indicated) were prepared in cleavage buffer [10 mM Tris–HCl, pH 7.5, 10 mM $MgCl_2$, 5 μg/ml bovine serum albumin (BSA), 50 mM NaCl—unless otherwise indicated], with 1 mM of freshly prepared dithiothreitol (DTT).

Cas12a protein and crRNA were complexed by directly mixing crRNA (in IDTE buffer) with Cas12a (in storage buffer, 20 mM Tris–HCl, pH 7.5, 500 mM NaCl, 50% glycerol, 1 mM DTT) and incubated at room temperature for 10 min. *Cis* cleavage was performed by addition of DNA target solution to a final concentration of 10 nM Cas12a, 20 nM crRNA, and 1 nM target dsDNA in 1× cleavage buffer (NaCl concentration as indicated). This *cis* cleavage reaction was incubated in a thermocycler at 30°C for strictly 20 min.

The *cis* cleavage reaction was then further diluted in appropriate 1× cleavage buffer, and 50 μl added to each well of a flat-clear-bottom black fluorescence 96-well plate (Thermo Fisher). Fluorescent-quencher reporter ssDNA was prepared in 1× cleavage buffer (NaCl as indicated, reporter ssDNA final concentration 75 nM), 50 μl of which was added into each well by multichannel pipette. Fluorescence over time for all assays was measured at 30°C for 60 min in a Victor Nivo (PerkinElmer) or an Infinite M Nano plate reader (Tecan), using the 480/30 nm filter for excitation and the 530/30 nm filter for emission.

Trans cleavage in the absence of target DNA or crRNA was performed in no-NaCl cleavage buffer and 500 nM reporter ssDNA. Reactions with a final concentration of ∼1 mM NaCl were attained by a total of 500-fold dilution across the steps of crRNA complexing, *cis* cleavage reaction, and addition of reporter ssDNA; the Cas12a proteins being stored in a buffer containing 500 mM NaCl.

Fluorescence curves were plotted using GraphPad Prism 10 (GraphPad Software). For pseudo-first-order *trans* cleavage kinetics, the first 300 s were extracted, and a linear regression was fitted to each replicate (GraphPad Software). Values of fluorescence increase per second (ΔFs^{-1}) were then plotted (GraphPad Software).

Cis cleavage kinetics

These were performed as previously described [12], with the exception of FnCas12a WT kinetics performed in cleavage buffers containing final concentrations of ∼1, 100, or 200 mM NaCl, as indicated.

Briefly, Cas12a–crRNA complexes (cognate DNMT1-3 crRNA, Supplementary Table S2) were assembled and incubated with a target plasmid for set time intervals. The obligatory sequential NTS and then TS cleavage mechanism of Cas12a causes changes in plasmid DNA topology, from negatively supercoiled to the 'nicked' open-circle, and finally to the linearized form [12, 14, 15]. These changes in topology are visible by agarose gel electrophoresis [23], and supercoiled, nicked, and linearized fractions were quantified by ImageJ

Downloaded from https://academic.oup.com/nar/article/54/1/gkaf1485/8418215 by guest on 26 March 2026

[24]. Fitting of a sequential strand cleavage model to changes in DNA topology over time was used to derive rate constants of NTS and TS cleavage [12, 14, 15].

DNA detection experiments

Cas12a–crRNA complexes were prepared as for *trans* cleavage kinetics. Complexes were diluted in 1× cleavage buffer to 10 nM (final NaCl concentration as indicated), and 10 µl added per well (Applied Biosystems MicroAmp Optical 96-well Reaction Plate, Thermo Fisher). 'DNA reporter' solution was prepared, containing a final concentration of 200 mM fluorescent-quencher reporter ssDNA and 50 pM target dsDNA in 1× cleavage buffer (final NaCl concentration as indicated). Ten microliters of DNA solution was added to the 96-well plate (on ice) using a multichannel pipette and mixed well. The plate was covered with adhesive film (MicroAmp Optical, Thermo Fisher) and loaded into an Applied Biosystem quantitative-PCR machine. Fluorescence values were recorded every 30 s, and curves were plotted in GraphPad Prism 10 (GraphPad Software). Statistical tests on endpoint fluorescence values at 30 min were performed to assess DNA detection ability, using two-way ANOVA followed by Tukey's multiple comparisons test in GraphPad Prism 10 (GraphPad Software).

DNA detection in human saliva was performed as above, with the following modifications. The DNase activity of saliva was inactivated by the addition of 2% (v/v) Proteinase K (Bioline), with incubation at 55°C for 10 min, then 98°C for 10 min. A final concentration of 150 nM ssDNA reporter was used in 1× cleavage buffer (with no added NaCl), and the remaining 63% of sample volume consisted of human saliva (Innovative Research Inc. Pooled Human Saliva 5 ml, Thermo Fisher).

Genome editing of cell lines

Three replicate editing experiments were performed per nuclease, precisely as previously described [12]—with the following addition. Positive control consisting of 30 pM Alt-R AsCas12a Ultra (IDT) was complexed with 0.575 µM DNMT1-3 crRNA and complexed as previously described [12]. This was then delivered by electroporation into HEK293T, A549, and Jurkat cells. Cell culturing, electroporation, genomic DNA extraction, and high-throughput sequencing were then performed precisely as described [12]. Statistical significance of gene editing was performed on the percentage of insertions/deletions (indels), using two-way ANOVA followed by Tukey's multiple comparisons test in GraphPad Prism 10 (GraphPad Software).

Results

Alanine substitution near the RuvC can abolish the *trans* cleavage of Cas12a orthologues

We first generated alanine substitutions of a conserved arginine in the Nuc domain (FnR1218, AsR1226, and LbR1138, Fig. 1 A–C) that is critical for *cis* and *trans* cleavage [4, 7, 8]. We determined the *cis* cleavage kinetics of these mutants and replicated previous results showing globally depressed rates of NTS and TS cleavage, with no detectable *trans* cleavage activity (Supplementary Fig. S1) [4, 8, 11, 25].

We next wondered whether other nearby positively charged residues had similar effects on DNA cleavage. We identified a lysine residue (FnK1084, AsK1072, LbK1003) adjacent to the conserved arginine (FnR1218, AsR1226, LbR1138). Mapping the Coulombic electrostatic potential onto the RuvC and Nuc domains showed this amino acid, and several others, contribute to the positive charge of the protein surface near the active site cleft (Fig. 1A–C and Supplementary Figs S2--S4).

Alanine substitution of K1084 in FnCas12a was sufficient to reduce *trans* cleavage to near undetectable (Fig. 1D and Supplementary Fig. S5A). This was not the case for the orthologous substitution in AsCas12a (K1072A; Fig. 1E and Supplementary Fig. S5B), nor in LbCas12a (K1003A; Supplementary Fig. S5C). We generated single, double, triple, and quadruple alanine substitutions to achieve Cas12a mutants with severely reduced *trans* cleavage activity (Fig. 1D–F). For AsCas12a, the triple alanine substitution mutant '3×A' (K1072A/K1086A/R1220A) exhibited the weakest *trans* cleavage activity (Fig. 1E and Supplementary Fig. S5B); for LbCas12a, it was the quadruple alanine substitution mutant '4×A' (K1003A/K1015A/K1017A/R1054A; Fig. 1F and Supplementary Fig. S5C and D). We next assayed the *cis* cleavage kinetics of these mutants (Supplementary Fig. S6 and Supplementary Table S3). NTS and TS cleavage of FnCas12a K1084A reduced by 1.8- and 1.3-fold, while AsCas12a '3×A' reduced 2.1- and 7-fold, respectively (Supplementary Fig. S7 and Supplementary Table S3). NTS cleavage by LbCas12a mutants was mildly affected, reduced 1.5- to 2.1-fold from double to quadruple alanine substitution mutant (Supplementary Fig. S7 and Supplementary Table S3). TS cleavage was less affected, slowed by 1.1- to 1.5-fold (Supplementary Fig. S7 and Supplementary Table S3).

We reasoned that these alanine substitution mutants lose *trans* cleavage activity through loss of electrostatic interactions between positive charges on the surface of the Nuc domain and the negatively charged backbone of substrate DNA. This is consistent with numerous reports showing decreased *trans* cleavage rates with increasing ionic strength in reaction buffers [3, 19, 20]. We replicated this effect in reaction buffers ranging from ∼1 to 100 mM NaCl (Supplementary Figs S8 and S9). Here, the higher NaCl concentration slows *trans* cleavage, and lower NaCl concentrations allow increasing rates of *trans* cleavage.

This effect varied between Cas12a orthologues, with LbCas12a the least affected by increasing NaCl concentration (Supplementary Figs S8 and S9). This effect is consistent with our mutagenesis study, where LbCas12a required four alanine substitutions to abolish *trans* cleavage, while for FnCas12a and AsCas12a, one and two substitutions were sufficient to suppress most *trans* cleavage activity (Fig. 1D–F). Given a single alanine substitution could effectively abolish the *trans* cleavage of FnCas12a, and *trans* cleavage could be well suppressed by high NaCl concentration, we explored the effect of NaCl concentration on the *cis* cleavage kinetics of FnCas12a. We found that *cis* cleavage rates did not greatly change across 1–200 mM NaCl, with k_{NTS} and k_{TS} varying by 1.6- to 1.3-fold, respectively (Supplementary Figs S10 and S11 and Supplementary Table S3). More important was alanine substitution of residues near the RuvC, with the FnK1084A/K1098A double mutant having 1.7-fold reduced k_{NTS} and 2.7-fold slower k_{TS} (Supplementary Fig. S11 and Supplementary Table S3).

To further test our defectively *trans*-cleaving Cas12a mutants, we complexed them with a 'pre-cleaved' dsDNA

Downloaded from https://academic.oup.com/nar/article/54/1/gkaf1485/8418215 by guest on 26 March 2026

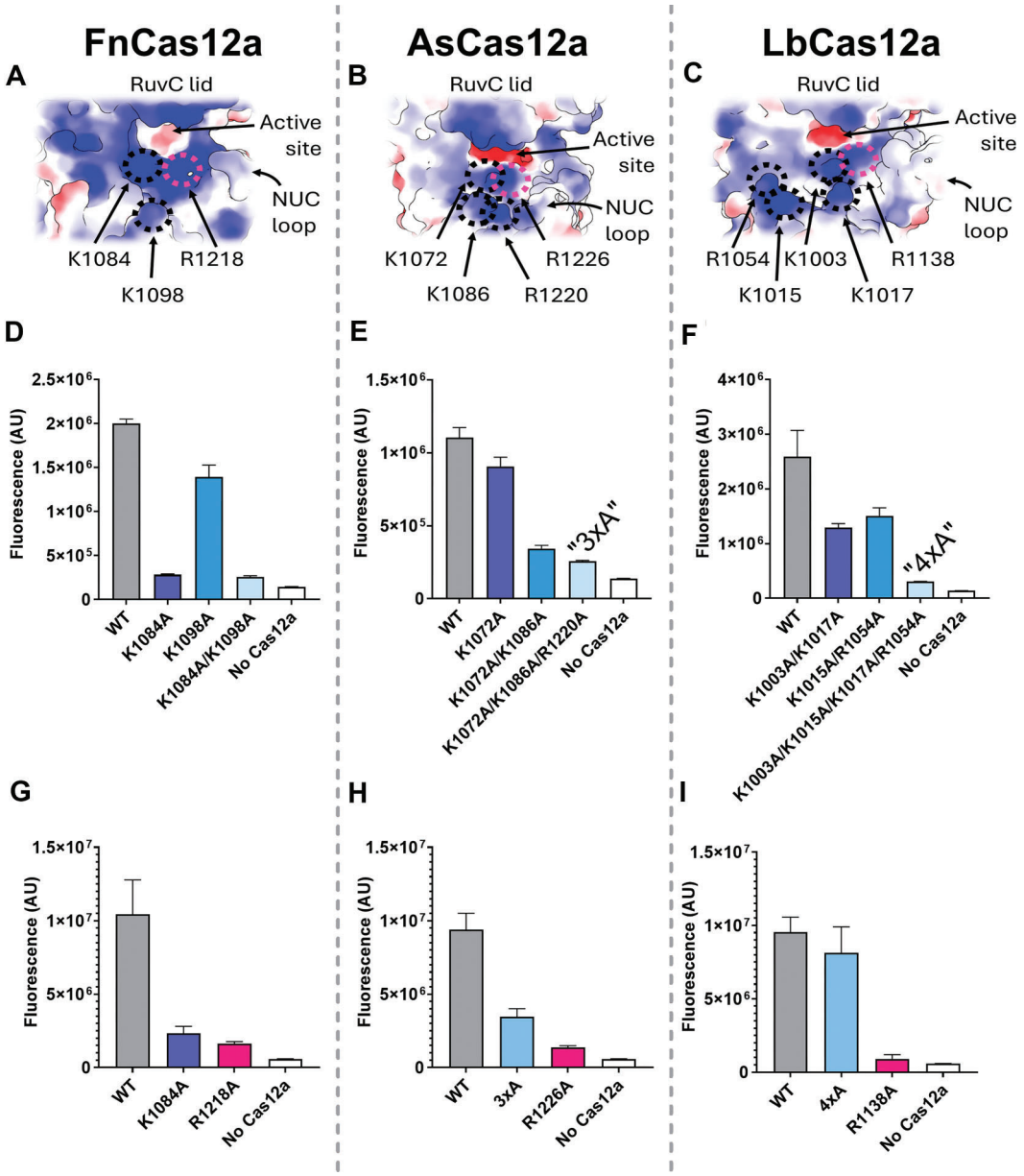


Figure 1. Coulombic electrostatic potential mapped onto the surface of (**A**) FnCas12a (GTG), (**B**) AsCas12a (8SFR), and (**C**) LbCas12a (A0A182DWE3AFDB prediction to show incomplete lid and Nuc-loop). Electrostatic potential is displayed on a colour gradient showing negative (red), neutral (white), and positive (blue). Arrows show the RuvC active site cleft, Nuc loop, and key amino acids that contribute to positive surface charge. Endpoint fluorescence after 60 min *trans* cleavage reaction, when activated with 1 nM target dsDNA, for wild-type and mutants of (**D**) FnCas12a, (**E**) AsCas12a, and (**F**) LbCas12a. Endpoint fluorescence after 60 min *trans* cleavage reaction, when activated with 1 nM 'pre-cleaved' dsDNA substrate, for WT and low-*trans* cleavage mutants of (**G**) FnCas12a, (**H**) AsCas12a, and (**I**) LbCas12a.

substrate containing a 20 nt TS and 14 nt NTS and tested their *trans* cleavage in the low salt condition (~1 mM NaCl; Fig. 1G–I and Supplementary Fig. S12). This assay showed that single mutants K1084A and R1218A of FnCas12a have very little affinity to the ssDNA *trans* substrate (Fig. 1G and H and Supplementary Fig. S12B and C). AsCas12a mutant '3×A' retained very weak *trans* cleavage, while the LbCas12a '4×A' retained the most *trans* cleavage activity (Fig. 1H and Supplementary Fig. S12D). The '4×A' mutant had a significantly slower increase in fluorescence, despite reaching similar values to WT LbCas12a after 60 min, indicating this mutant was significantly impaired in its *trans* cleavage activity.

That this '4×A' mutant of LbCas12a retained some degree of *trans* cleavage suggested that the LbR1138 residue alone could mediate this activity, unlike the R1218 of FnCas12a or R1226 of AsCas12a. In the allosteric activation of the RuvC active site, the occluding lid loop opens and closes [9]. We reasoned that LbCas12a may have intrinsically faster rates of 'opening' the RuvC lid, relative to FnCas12a and AsCas12a. The lid contains a conserved phenylalanine that base-stacks with incoming nucleic acids (Fn F1012, As F999, Lb F931) and aids their coordination in the RuvC alongside the network of positively charged Nuc residues. So, we analysed the structures of the RuvC lid of Cas12a orthologues.

Downloaded from https://academic.oup.com/nar/article/54/1/gkaf1485/8418215 by guest on 26 March 2026

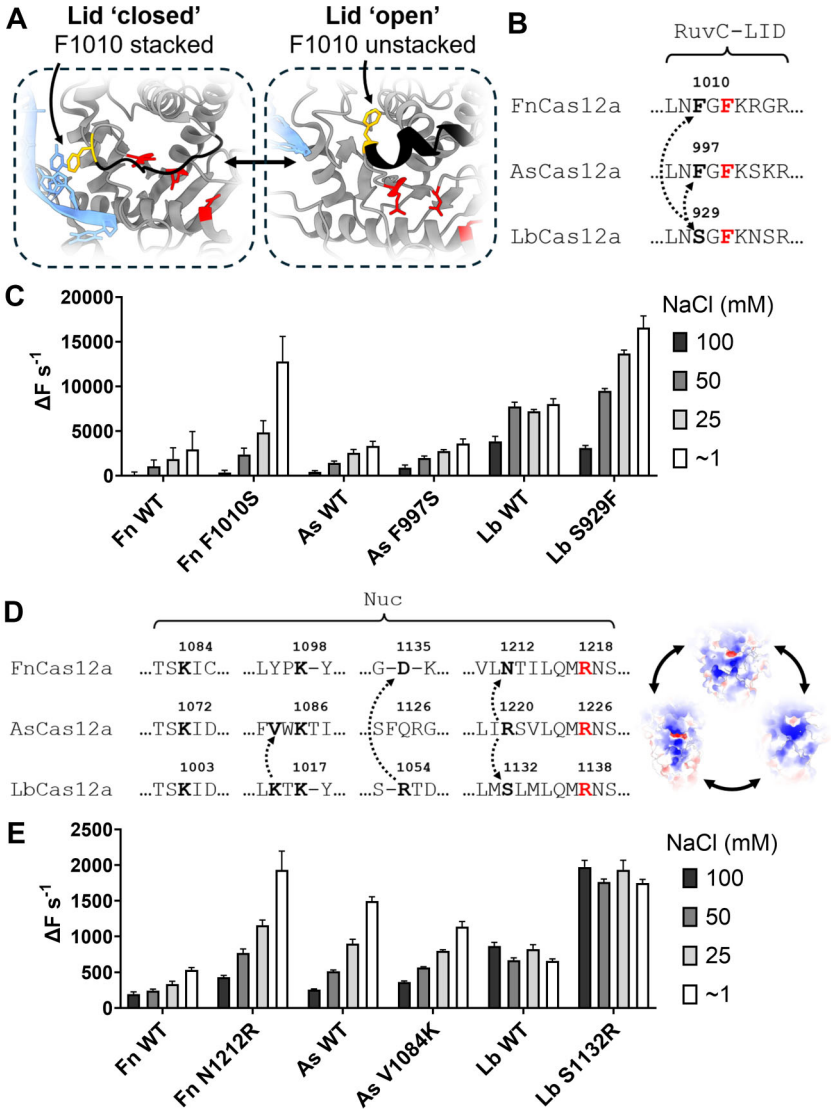


Figure 2. (**A**) Diagram of the RuvC active site of FnCas12a, with catalytic residues shown in red. Polypeptide is shown in grey, while the lid motif is shown in black. Left box shows the RuvC lid of FnCas12a in the closed state (PDB: 6I1K), and the right box in the open state (PDB: 6GTG). Residue F1010 (mustard yellow) is shown interacting with the non-target DNA strand (blue) in the closed state. (**B**) Alignment of RuvC lid of FnCas12a, AsCas12a, and LbCas12a, with conserved lid–phenylalanine residue in bold red. Amino acids substituted in bold. (**C**) *Trans* cleavage rates of WT Cas12a and mutants, as quantified by the initial slope of the fluorescence curve. *Trans* cleavage reactions performed in buffers with final concentration of NaCl from ~1 to 100 mM. (**D**) Schematic of orthologue-informed mutagenesis. Selected alignment of Nuc domains of FnCas12a, AsCas12a, and LbCas12a, with mutated residues in bold. Conserved RuvC-proximal arginine in red. (**E**) *Trans* cleavage rates of WT Cas12a and mutants, as quantified by the initial slope of the fluorescence curve. *Trans* cleavage reactions performed in buffers with final concentration of NaCl from ~1 to 100 mM.

Lid and Nuc substitutions can increase the *trans* cleavage activity of Cas12a orthologues

In analysing structures of Cas12a, we noted that a lid-NTS stacking interaction was present in the closed-lid conformation of FnCas12a (Fig. 2A). Here, F1010 of FnCas12a forms a stacking interaction with the 11th nucleotide of the non-target DNA strand [11]. This stacking between F1010 and the NTS was not present in structures showing the 'open' lid conformation (Fig. 2A) [26]. Alignment of the RuvC lid between Cas12a orthologues showed that LbCas12a harbour a serine in this position, unlike the phenylalanine of FnCas12a and AsCas12a. We hypothesized that removing the possibility of lid-NTS stacking may promote the open lid conformation, increasing *trans* cleavage.

To test this hypothesis, we generated orthologue-informed substitutions, whereby the serine of LbCas12a replaced the phenylalanine of FnCas12a and AsCas12a, and vice versa (Fig. 2B), and tested their *trans* cleavage in the ~1 to 100 mM NaCl conditions. FnCas12a F1010S had increased *trans* cleavage relative to WT, which was more pronounced at ~1 and 25 mM NaCl (Fig. 2C and Supplementary Fig. S13). AsCas12a F997S exhibited similar rates of *trans* cleavage to WT (Fig. 2C and Supplementary Fig. S14). We expected the LbCas12a mutant S929F would show decreased cleavage activity; however, we observed increased *trans* cleavage rates (Fig. 2C and Supplementary Fig. S15). The increase in *trans* cleavage was notable in the ~1 and 25 mM NaCl conditions and not apparent at 50 and 100 mM NaCl (Fig. 2C and Supplementary Fig. S15).

Encouraged by the possibility of engineering Cas12a nucleases with increased *trans* cleavage, we generated orthologue-informed substitutions of the Nuc domain, this time to

Downloaded from https://academic.oup.com/nar/article/54/1/gkaf1485/8418215 by guest on 26 March 2026

introduce positively charged amino acids where an orthologue was lacking (Fig. 2D). We chose positions shown to be important for *trans* cleavage in Fig. 1. For example, residue R1220 of AsCas12a aligns structurally with FnCas12a N1212 and LbCas12a S1132. Likewise, LbCas12a R1054 aligns with AsCas12a V1084. Thus, we substituted these amino acids for arginine or lysine.

We generated mutations of the Nuc domain and tested their *trans* cleavage across the ∼1 mM to 100 mM NaCl conditions. Mutation N1212R for FnCas12a improved *trans* cleavage rates across NaCl concentrations, while V1084K substitution for AsCas12a showed a very slight improvement at 100 mM NaCl (Fig. 2E and Supplementary Figs S16 and S17). For LbCas12a, the S1132R mutation consistently improved *trans* cleavage rates across NaCl concentrations (Fig. 2E and Supplementary Fig. S18). Substitution mutant D1135K for FnCas12a exhibited *trans* cleavage rates comparable to WT in ∼1 to 50 mM and slightly increased at 100 mM NaCl (Supplementary Fig. S19). Double mutants FnF1010S/N1212R and FnD1135K/N1212R showed increased *trans* cleavage, while the triple mutant F1010S/D1135K/N1212R, or 'SKR', showed the highest *trans* cleavage activity (Supplementary Fig. S20).

Engineered Cas12a nucleases show enhanced *cis* cleavage and DNA detection

We next assayed the *cis* cleavage kinetics of single and combination mutants (Supplementary Figs S21 and S22). Single mutants of FnCas12a exhibited rates of NTS and TS cleavage similar to WT, while double mutants F1010S/N1212R and D1135K/N1212R had decreased rates of k_{NTS} and k_{TS}, respectively (Fig. 3A and Supplementary Table S3). Triple mutant 'SKR' showed increased k_{NTS} relative to WT and similar k_{TS} (Fig. 3A, Supplementary Table S3). AsCas12a F997S had similar *cis* cleavage kinetics to WT, while the V1084K mutation decreased k_{NTS} by 4.5-fold and increased k_{TS} by 1.6-fold (Fig. 3B and Supplementary Table S3). LbCas12a S929F mutant exhibited a 2.5-fold increase in k_{NTS} relative to WT, while S1132R substitution increased k_{TS} by 2.6-fold (Fig. 3B and Supplementary Table S3). Combination mutant S929F/S1132R increased k_{NTS} by 2.1-fold and k_{TS} by 1.3-fold (Fig. 3B and Supplementary Table S3). We further assessed the effect of mutations on protein thermostability, which determined single and combination mutants of Cas12a orthologues have similar-to-WT stability (Supplementary Fig. S23).

Engineered Cas12a mutants have additional positive charges in their Nuc domains. We hypothesized these mutants would show increased *trans* cleavage at higher ionic strengths. We tested this hypothesis using an HPV16 crRNA and matching dsDNA target across 50–200 mM NaCl (Fig. 3C and Supplementary Fig. S24). FnCas12a triple mutant 'SKR' showed increased *trans* cleavage rates at 50 to 100 mM NaCl, with both WT and mutant having very slow *trans* cleavage at 200 mM (Fig. 3C and Supplementary Fig. S24). AsV1084K had similar *trans* cleavage rates to WT at 200 mM NaCl and increased at 50 to 100 mM (Fig. 3C and Supplementary Fig. S24). Double mutant LbS929F/S1132R had similar to WT rates of *trans* cleavage, but increased at the 200 mM condition (Fig. 3C and Supplementary Fig. S24).

We next tested these engineered Cas12a nucleases for their ability to detect low concentrations of DNA. To illustrate the effect of monovalent ions on *trans* cleavage, we conducted this assay in both ∼1 and 50 mM NaCl conditions, with the low-salt condition generally resulting in higher endpoint fluorescence (Fig. 3D and E and Supplementary Figs S25 and S26). Engineered nucleases typically outperformed wild-types, with the exception of LbCas12a WT and S929F/S1132R, which both displayed very robust DNA detection (Fig. 3D and E and Supplementary Figs S25 and S26). Unlike FnCas12a and LbCas12a nucleases, AsCas12a WT and mutants had relatively high rates of *trans* cleavage in the absence of crRNA or target DNA, limiting their DNA detection sensitivity (Supplementary Fig. S27). Consistent with previous reports, we found this activity is mediated by *apo* AsCas12a, as it decreases with molar excesses of crRNA (Supplementary Fig. S28). Finally, we performed DNA detection in a sample matrix of 63% human saliva (Fig. 3F and Supplementary Figs S29 and S30). Endpoint fluorescence values were lower, and only LbCas12a WT and S929F/S1132R had significantly increased fluorescence compared to the no-DNA control, with S929F/S1132R outperforming WT LbCas12a (Fig. 3F and Supplementary Fig. S30).

Finally, we tested the genome editing efficiency of high- and low-*trans* cleaving Cas12a mutants of AsCas12a and LbCas12a. FnCas12a WT and variants were not tested due to their established low activity in genome editing [5, 27]. We chose three human cell lines commonly used for genetic engineering and cell-based assays—HEK293T, A549, and Jurkat. We electroporated Cas12a complexed to crRNA targeting either the DNMT1-3, DNMT1-7, or AGBL1 genes, and insertions or deletions (indels) were assessed by high-throughput sequencing.

Cas12a mutants with low-*trans* cleavage typically showed reduced indels, while high-*trans* cleavage mutants had retained or increased editing relative to WT (Fig. 4). AsCas12a triple mutant '3×A' had significantly reduced indel activity at the DNMT1-3 site across all three cell lines tested. Mean indels for WT and mutants were lower overall at the DNMT1-7 and AGBL1 sites, but the '3×A' mutant had consistently lower-than-WT editing activity (Fig. 4A, C, and E). AsV1084K had editing efficiencies similar to WT across all cell lines and target sites and significantly higher at the DNMT1-3 site in HEK293T cells (Fig. 4A). The LbCas12a '4×A' mutant had similar or lower editing efficiency to WT LbCas12a, while the S929F/S1132R mutant had similar or increased activity (Fig. 4B, D, and F). This increase was only weakly significant at the DNMT1-7 site in Jurkat cells (Fig. 4F). We also assessed editing at previously identified off-target sites (Supplementary Figs S31--S33) [27]. All nucleases showed no significant increase in off-target editing—with the exception of AsV1084K—which exhibited increased editing at off-target site 1 with the DNMT1-3 crRNA in A549 and Jurkat cells (Supplementary Figs S32 and S33). This off-target editing reached a maximum of 3% indels (Supplementary Fig. S32).

We further compared our engineered nucleases by comparison with a commercially available Cas12a variant—AsCas12a 'Ultra' [28]. We compared on- and off-target editing using the DNMT1-3 crRNA across three cell lines (Supplementary Figs S34 and S35). AsCas12a 'Ultra' had significantly higher on-target indel activity than our nucleases in HEK293T and A549 cell lines, with similar but lower activity in Jurkat cells (Supplementary Fig. S34). However, AsCas12a 'Ultra' exhibited very high activity at the DNMT1-3 off-target-1, with 20% to 70% indels across all three cell lines tested (Supplementary Fig. S35).

Downloaded from https://academic.oup.com/nar/article/54/1/gkaf1485/8418215 by guest on 26 March 2026

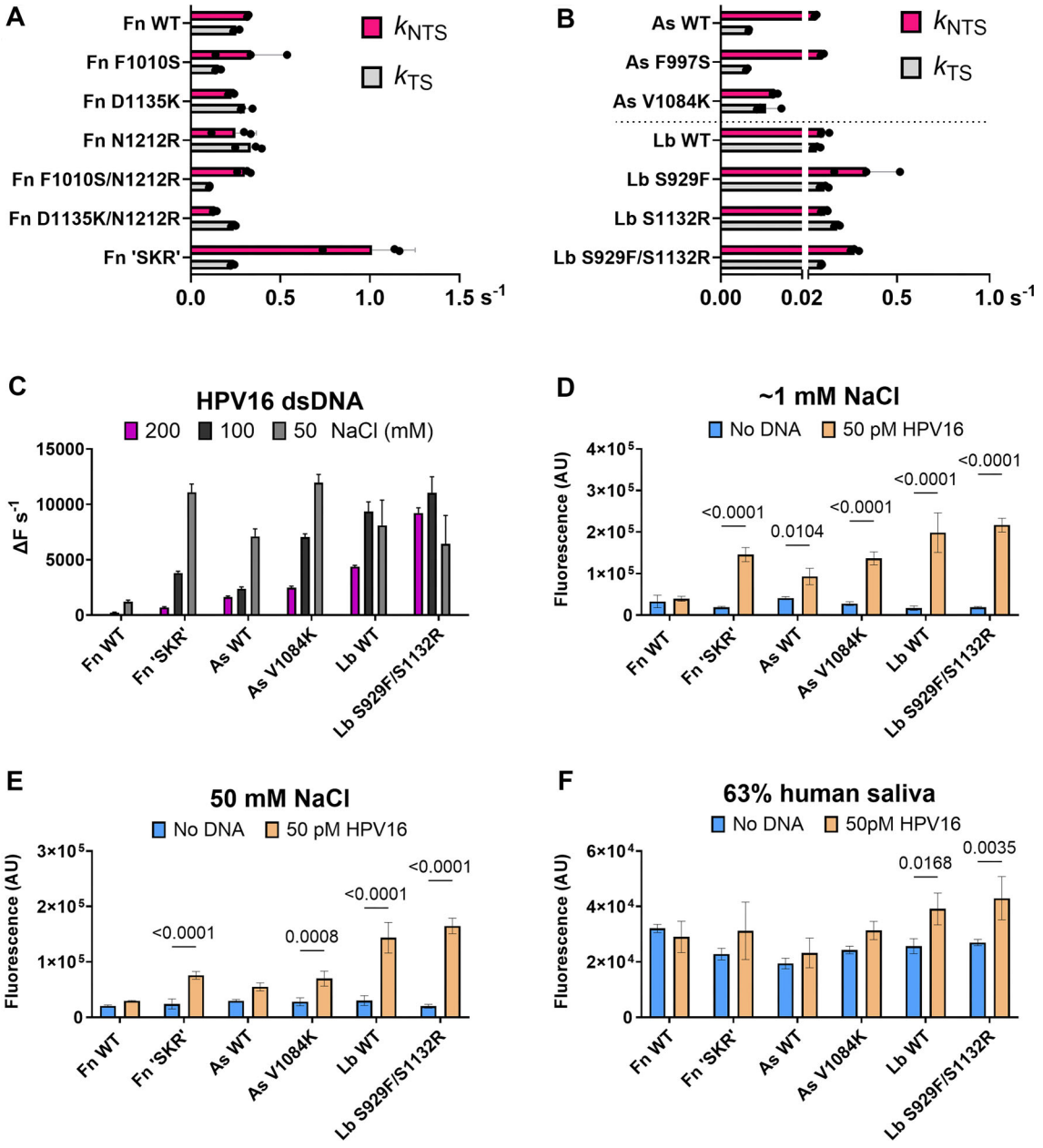


Figure 3. (**A, B**) Kinetic values (s^{-1}) of NTS (k_{NTS}, pink) and TS cleavage (k_{TS}, grey), for the Cas12a indicated. Dots show individual replicates, bars show mean, and error bars show s.d. (**C**) *Trans* cleavage rates with HPV16 dsDNA target in 50, 100, and 200 mM NaCl, as quantified by the initial slope of fluorescence curve. (**D**) Detection of 50 pM HPV16 dsDNA by endpoint fluorescence at 30 min in ∼1 mM final concentration of NaCl. (**E**) Detection of 50 pM HPV16 dsDNA by endpoint fluorescence at 30 min in 50 mM final concentration of NaCl. (**F**) Detection of 50 pM HPV16 dsDNA by endpoint fluorescence at 30 min in sample that is 63% (*v/v*) human saliva. Statistical significance evaluated by two-way ANOVA with Tukey's multiple comparison test, with *P*-values shown above bars.

Discussion

The *trans* cleavage activity of Cas12a has been widely employed for molecular detection. Here, we show that electrostatic interactions are key drivers of the *trans* cleavage activity of Cas12a orthologues. This finding rationalizes the high *trans* cleavage activity seen with low-salt buffers and formed the basis of engineering improved Cas12a variants.

Nuc electrostatics are critical for the *trans* cleavage of Cas12a orthologues

We replicated previous findings that FnR1218A, AsR1226A, and LbR1138A had highly impaired *cis* cleavage kinetics (3 to 6 orders of magnitude slower than WT) and no detectable *trans* cleavage (Supplementary Fig. S1). We further determined that these mutants were unable to effect *trans* cleavage even when complexed to a pre-cleaved dsDNA substrate in a no-NaCl reaction buffer (Fig. 1G–I). This indicates this residue provides critical affinity to *trans* substrate ssDNA (Fig. 5).

Alanine substitution of other lysine and arginine residues near the RuvC had variable effects on *cis* and *trans* cleavage across Cas12a orthologues (Fig. 1D–F and Supplementary Figs S5--S7). This is likely due to different exact protein–nucleic acid interactions Cas12a orthologues employ to bind and cleave *cis* and *trans* substrates. The NTS and TS are

Downloaded from https://academic.oup.com/nar/article/54/1/gkaf1485/8418215 by guest on 26 March 2026

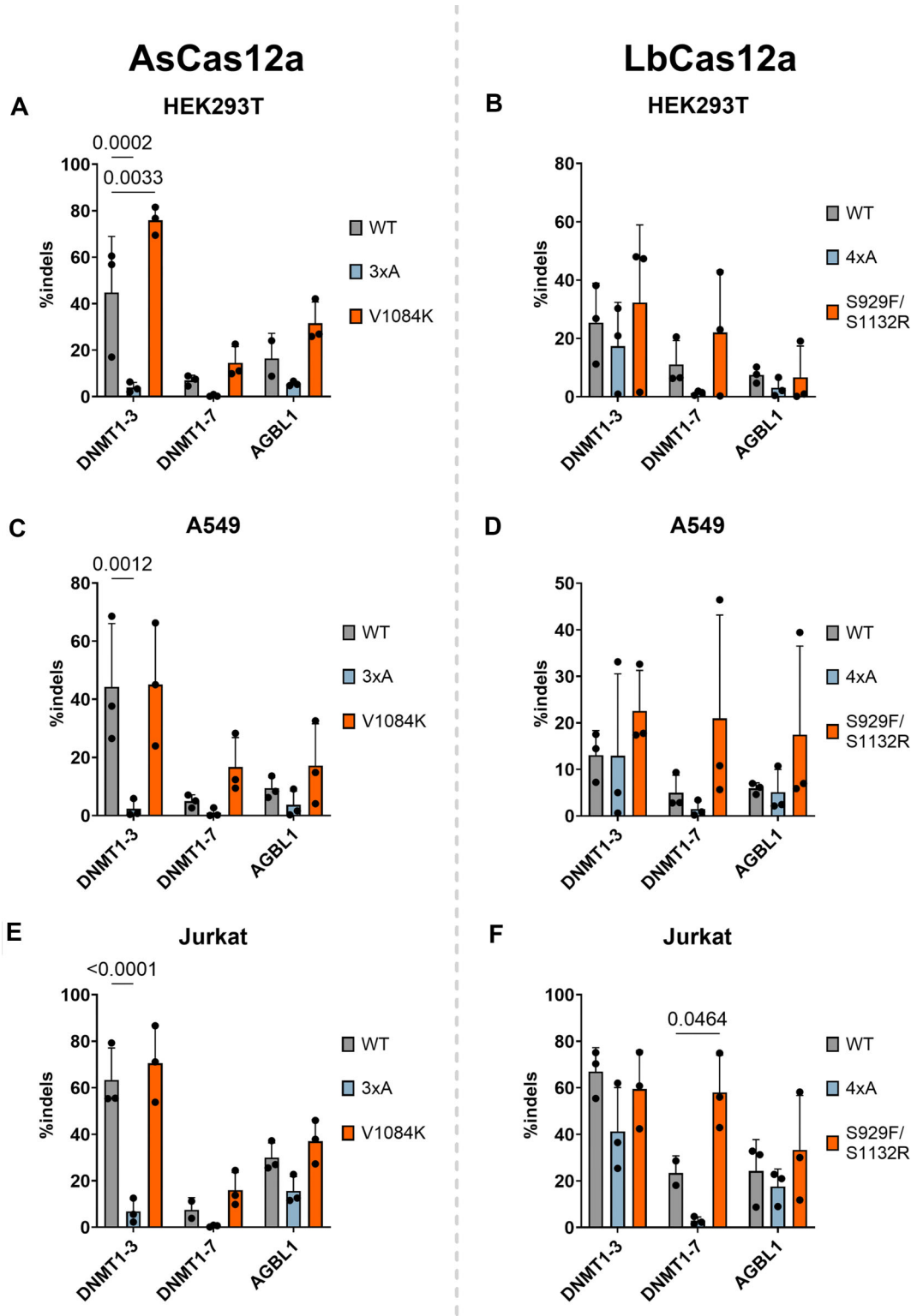


Figure 4. Genome editing in HEK293T cells by (**A**) AsCas12a and (**B**) LbCas12a nucleases. Genome editing in A549 cells by (**C**) AsCas12a and (**D**) LbCas12a nucleases. Genome editing in Jurkat cells by (**E**) AsCas12a and (**F**) LbCas12a nucleases. Statistical significance evaluated by two-way ANOVA with Tukey's multiple comparison test, with *P*-values shown above bars.

Downloaded from https://academic.oup.com/nar/article/54/1/gkaf1485/8418215 by guest on 26 March 2026

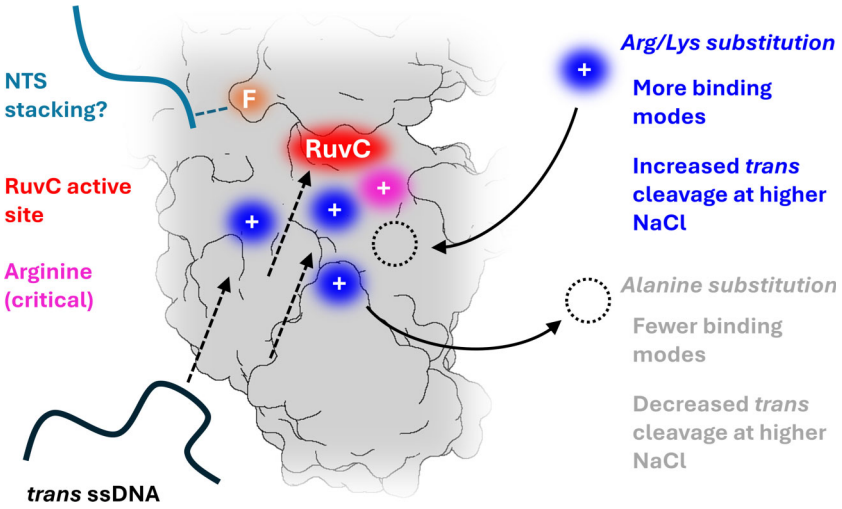


Figure 5. Model of Nuc electrostatics and *trans* cleavage, showing; putative stacking interaction between NTS (sea green) and RuvC lid phenylalanine (orange), RuvC active site cleft (red) with adjacent conserved and critical arginine residue (pink), positively charged residues (blue) that play a role in *trans* cleavage, which can be removed by alanine substitution (dashed circle), and *trans* ssDNA substrate (black) with arrows showing potential modes for binding and cleavage by Cas12a. FnCas12a (grey, PDB: 6GTG) is used as a generic representation of a NUC lobe; positions of key residues and nucleic acid substrates are representative only.

coordinated to Cas12a by numerous interactions across the REC and NUC lobes [7–9, 11, 17, 26], while *trans* substrate ssDNA is predicted to transiently interact with Nuc and RuvC domains [29]. We propose that this weaker interaction between *trans* substrate ssDNA and Cas12a underpins the greater loss of *trans* cleavage versus *cis* cleavage upon alanine substitution of Nuc residues—i.e. the single mutant FnK1084A abolishes *trans* cleavage while retaining *cis* cleavage rates within two-fold of WT (Supplementary Figs S5A and S7). Similarly, changing NaCl concentrations in reaction buffers from 1–200 mM NaCl had relatively little effect on the *cis* cleavage of FnCas12a WT, unlike what was observed for *trans* cleavage (Supplementary Figs S8--S11).

AsCas12a single mutants K1072A and K1086A reduced *trans* cleavage rates relative to WT, the double mutant further reduced *trans* cleavage, and triple combination mutant with R1220A—'3×A'—having the weakest *trans* cleavage activity (Supplementary Fig. S5B). We suggest that R1226, K1072, and K1086 are the major contributors to *trans* substrate binding, with some contribution of R1220. We suggest these residues also contribute significantly to *cis* substrate binding, the '3×A' mutant having 2.1-fold lower k_{NTS} and 7-fold slower k_{TS} compared to AsCas12a WT (Supplementary Fig. S7).

LbCas12a single mutants of K1003A and R1054A reduced *trans* cleavage to a greater extent than K1015A and K1017A (Supplementary Fig. S5C). Double mutants including K1003A were more impaired in *trans* cleavage than double mutants not including it—i.e. K1015A/K1017A and K1015A/R1054A (shown in bold, Supplementary Fig. S5C). This would suggest *trans* ssDNA substrates bind to R1138 and K1003 in conjunction with other positively charged residues—i.e. K1015, K1017, or R1054. The LbCas12a '4×A' mutant retained a degree of *trans* cleavage when incubated with a pre-cleaved *cis* substrate, compared to the minimal activity of FnCas12a K1084A and AsCas12a '3×A' (Supplementary Fig. S12). This would suggest the LbCas12a R1138 residue alone has reasonable affinity to *trans* substrate ssDNA. Indeed, despite the slower *cis* cleavage kinetics of LbCas12a '4×A' (Supplementary Fig. S7), this mutant displayed similar-to-WT levels of gene editing at some target sites, unlike the AsCas12a '3×A' mutant (Fig. 4).

Our alanine mutagenesis study of FnCas12a, AsCas12a, and LbCas12a indicates that electrostatic interactions of Nuc domain residues are critical for the *trans* cleavage of these orthologues (Fig. 5). Specifically, alanine substitution of positively charged residues closest to the active site cleft tends to have a larger negative effect on DNase activity, as does alanine substitution of multiple such residues of the Nuc.

These data provide a mechanistic basis for high *trans* cleavage observed in low-salt buffers [3, 16, 19, 20, 30]. Moreover, increased *trans* cleavage by LbCas12a has been observed with increasing pH [30, 31], which one would expect to yield fewer protonated lysine and arginine residues but a more deprotonated phosphate backbone of target ssDNA [32]. However, complex equilibria between the protonation state of nucleic acid-interacting residues, cation release from nucleic acids, and the entropic and enthalpic contributions of both have been previously observed for nucleic acid-binding proteins [33]. Future empirical studies could dissect the linkage between pH and monovalent ion concentrations to discover optimal buffer conditions for *trans* cleavage by Cas12a.

RuvC-lid and Nuc substitutions can generate Cas12a variants with enhanced *cis* and *trans* cleavage

We explored the role of RuvC-lid substitution in the *cis* and *trans* cleavage of Cas12a orthologues. It had been previously established that a conserved phenylalanine of the RuvC-lid makes key interactions with *cis* and *trans* substrates (FnF1012, AsF999, LbF931) [9, 18]. Alanine substitution at this position reduced the TS cleavage kinetics of FnCas12a and AsCas12a [18] and abolished *trans* cleavage for AsCas12a [9]. We tested a less-conserved lid residue seen to interact with the NTS (FnF1010, AsF997, LbS929) [11] and found inconsistent effects on *cis* and *trans* cleavage (Fig. 2C). Substitution mutant LbS929F exhibited increased *cis* and *trans* cleavage,

Downloaded from https://academic.oup.com/nar/article/54/1/gkaf1485/8418215 by guest on 26 March 2026

as did FnF1010S to a lesser extent, while AsF997S had little effect on *cis* and *trans* cleavage (Fig. 3A and B). These data make the mechanistic role of this position unclear. We suggest that increases in *trans* cleavage derive from faster *cis* cleavage, where the introduction or removal of the putative lid-stacking interaction stabilizes target dsDNA binding and increases the lifetime of *trans*-active ternary complexes.

Nuc substitution had unpredictable effects on the *cis* cleavage of FnCas12a. While single substitution mutants of FnCas12a had similar *cis* cleavage kinetics to WT, double mutant FnD1135K/N1212R had 2.4-fold decreased k_{NTS}, and FnF1010S/N1212R had 2.5-fold decreased k_{TS} (Fig. 3A). However, the triple mutant FnF1010S/D1135K/N1212R—'SKR'—exhibited ∼3-fold increased k_{NTS} and enhanced *trans* cleavage kinetics (Fig. 3A).

AsCas12a V1084K mutant had 1.6-fold increased k_{TS} with 4.6-fold lower k_{NTS} (Fig. 3B). This mutation may interfere with NTS loading into the RuvC by stabilizing DNA binding further from the active site. AsV1084K slightly increased *trans* cleavage in higher NaCl conditions, having a greater effect when activated by the HPV16 dsDNA target (Figs 2E and 3C). The LbS1132R mutant increased k_{TS} by 2.7-fold, with similar k_{NTS} (Fig. 3B), and consistently increased *trans* cleavage rates across NaCl conditions (Fig. 2E). The combination mutant LbS929F/S1132R had 2.6-fold increased k_{NTS} and 1.4-fold increased k_{TS} (Fig. 3B), with enhanced *trans* cleavage in higher NaCl concentrations (Fig. 3C).

In total, these data suggest that orthologue-informed substitutions can be used to enhance the DNase activities of Cas12a. Previous structure-guided engineering of Cas12a has focused on introducing positively charged amino acids to enhance PAM or crRNA-TS heteroduplex interactions [27, 34]. Here, we show that RuvC-lid and Nuc substitutions can enhance both *cis* and *trans* cleavage activity of FnCas12a, AsCas12a, and LbCas12a, suggesting this approach could be applicable to other Cas12a orthologues.

High-*trans* cleaving Cas12a variants can enhance DNA detection and genome editing

We tested high-*trans* cleaving variants of Cas12a for their ability to detect low amounts of target DNA. In the ∼1 and 50 mM NaCl conditions, FnCas12a 'SKR' and AsCas12a V1084K mutants had significantly better DNA detection than WT (Fig. 3D and E). However, in a more realistic sample matrix comprising 63% human saliva, these nucleases failed to generate a fluorescence signal different from the no-DNA control (Fig. 3F). LbCas12a S929F/S1132R and WT both had very robust DNA detection across the ∼1 and 50 mM NaCl conditions and could detect DNA spiked into the human saliva sample, with the LbS929F/S1132R mutant generating higher fluorescence (Fig. 3D, E, and F). This mutant had increased activity in higher NaCl concentrations (Fig. 3C), which may account for its improved activity in electrolyte-rich human saliva [35].

We also assessed the gene editing activity of high-*trans* cleavage variants. Although AsV1084K showed only a modest increase in *trans* cleavage compared to WT, it had similar or higher gene editing activity across all target sites and cell lines tested (Fig. 4A, C, and E). However, it also had higher off-target activity when using the DNMT1-3 crRNA (Supplementary Figs S32 and S33). This ∼1%–3% off-target editing was low in comparison to the engineered AsCas12a 'Ultra' variant, which had up to 70% indels at this off-target site (Supplementary Fig. S35). Similar to a previously engineered Cas12a variant—enAsCas12a—AsCas12a 'Ultra' has increased activity at both on- and off-target sites (Supplementary Figs S34 and S35) [27]. It would appear mutations that allow wider PAM motif recognition also stabilize some degree of off-target activity. This increase is generally modest and can be mitigated by careful dosing of the Cas12a–crRNA complex in gene editing experiments [28]. The increase in k_{TS}, *trans* cleavage, and off-target editing by AsV1084K would suggest this mutation non-specifically stabilizes the binding and cleavage of DNA strands.

When the *trans* cleavage of Cas12a was first characterized, there was some concern this indiscriminate DNase activity may be deleterious in living cells [2]. However, it has been demonstrated that the *trans* cleavage of AsCas12a or LbCas12a causes no detectable off-targets in mouse embryos [36]. Similarly, *trans* cleavage had no discernible effect on plasmid or phage interference in *Escherichia coli* [37, 38]. This is likely due to the protection of ssDNA by binding proteins [39], higher ionic strength [40], and lower available amounts of Mg^{2+} ions in living cells compared to *in vitro* [41]. Thus, the AsCas12a V1084K variant is unlikely to cause unwanted off-target genome editing through enhanced *trans* cleavage; instead, it is likely through stabilizing off-target DNA binding and *cis* cleavage.

For example, the high-*trans* LbCas12a S929F/S1132R mutant displayed similar gene-editing activity to WT and significantly higher in one instance (Fig. 4B, D, and F), with consistently low off-target activity (Supplementary Fig. S31--S33). This modest effect would suggest these mutations make a minor difference in living cells.

Implications for high- and low-*trans* cleaving Cas12a variants

With an explosion of discovery and characterization of a variety of Cas12a orthologues and their use in molecular detection and genome editing [5, 42, 43], the ability to modulate *cis* and *trans* cleavage may be widely useful. For example, recent engineering of the NTS-binding groove of a thermostable Cas12a orthologue was able to increase its *trans* cleavage for more sensitive RT-LAMP-enabled detection of RNA [16]. Further engineering of the Nuc and RuvC-lid of this orthologue has the potential to further enhance its activity.

Modulating the *cis* and *trans* cleavage kinetics of Cas12a orthologues has practical implications in 'one-pot reactions' combining target amplification with Cas12a detection, which require slower *cis* cleavage to avoid depletion of target amplicons [44]. While this could be achieved by engineering a Cas12a variant with slower *cis* cleavage and faster *trans* cleavage, a successful alternate strategy is to use non-consensus PAM motifs to slow *cis* cleavage [44]. In this case, slow PAM binding would limit the *cis* cleavage of a highly active Cas12a variant, which could then unleash high rates of *trans* cleavage activity.

Although *trans* cleavage is central to generating a signal in Cas12a molecular detection, recent work has emphasized the importance of enzyme activation kinetics [45]. Before *cis* or *trans* cleavage, a Cas12a–crRNA binary complex must locate the target sequence by non-specific DNA diffusion and specific PAM motif binding [46]. This step is rate-limiting in detecting low-abundance DNA targets, and faster activation kinetics of

Downloaded from https://academic.oup.com/nar/article/54/1/gkaf1485/8418215 by guest on 26 March 2026

a Cas12a orthologue from *Thiomicrospira* sp. Xs5 (TsCas12a) generated a signal faster than LbCas12a [45]. This orthologue is more active than LbCas12a from 20 to 37°C, despite higher steady-state *trans* cleavage for the latter [45]. Orthologue-informed mutation of the Nuc domain of TsCas12a may enhance its steady-state *trans* cleavage for more sensitive room-temperature diagnostics [45].

Mutations that decreased *trans* cleavage could also decrease *cis* cleavage. This is likely by decreasing the strength of non-specific protein-nucleic acid interactions near the RuvC. This could be leveraged to improve the gene editing specificity of Cas12a orthologues. The specificity of Cas12a has been previously improved by weakening interactions between the REC lobe and the crRNA-TS heteroduplex [27]. The effect of alanine substitution mutants in the Nuc domain could be explored in a similar fashion. Although our triple and quadruple alanine substitution mutants of AsCas12a and LbCas12a had overall lower on-target gene editing activity (Fig. 4), it is possible that single or double mutants could retain more on-target activity.

Conclusions

In this work, we studied the role of the residues near the RuvC on the *cis* and *trans* DNA cleavage activities of three Cas12a orthologues. We found that alanine substitution of arginine or lysine residues in the Nuc domain can abolish the *trans* cleavage of Cas12a orthologues while modestly reducing *cis* cleavage rates. We replicated findings in the literature that increasing NaCl concentration in reaction buffers decreases *trans* cleavage rates and suggest these ions neutralize electrostatic interactions between positively charged Nuc residues and the negatively charged phosphate backbone of *trans* substrates. As these electrostatic interactions are critical, substituting additional arginine or lysine residues in the Nuc was able to increase *trans* cleavage rates, especially at higher ionic strengths. Substitutions of the RuvC-lid could also increase *trans* cleavage, but not predictably. Testing combinations of RuvC-lid and Nuc mutations yielded high- and low-*trans* cleaving variants of three Cas12 orthologues. This study provides a blueprint for future rational engineering of the *cis* and *trans* cleavage activity of Cas12a nucleases.

Acknowledgements

The authors would like to thank the Biomolecular Resource Facility at the ANU for undertaking the DNA sequencing.

Author contributions: Anthony Newman (Conceptualization [equal], Funding acquisition [supporting], Investigation [lead], Methodology [lead], Writing – original draft [equal], Writing – review & editing [equal]), Lora Starrs (Investigation [supporting], Resources [lead], Writing – original draft [supporting], Writing – review & editing [supporting]), and Gaetan Burgio (Conceptualization [equal], Funding acquisition [lead], Project administration [lead], Supervision [lead], Writing – original draft [equal], Writing – review & editing [equal]).

Supplementary data

Supplementary data is available at NAR online.

Conflict of interest

A.N. and G.B. declare no conflict of interests.

Funding

This work was supported by the National Health and Medical Research Council - NHMRC - (APP 2018833 and 2027987) (G.B.), and The Gordon and Gretel Bootes foundation (A.N.). This research was undertaken with the assistance of resources from the National Computing Infrastructure (NCMAS and ANUMAS schemes to G.B), an NCRIS enabled capability supported by the Australian Government. A.N. was supported by an Australian Government Research Training Program scholarship. Funding to pay the Open Access publication charges for this article was provided by the NHMRC (APP 2018833 and 2027987).

Data availability

Data from high-throughput sequencing have been deposited with the National Center for Biotechnology Information Sequence Read Archive under BioProject ID PRJNA1281281. All other datasets are available on request.

References

1. Kaminki MM, Abudayyeh OO, Gootenberg JS *et al.* CRISPR-based diagnostics. *Nat Biomed Eng* 2021;5:643–56. https://doi.org/10.1038/s41551-021-00760-7
2. Chen JS, Ma E, Harrington LB *et al.* CRISPR-Cas12a target binding unleashes indiscriminate single-stranded DNase activity. *Science* 2018;360:436–9. https://doi.org/10.1126/science.aar6245
3. Fuchs RT, Curcuru J, Mabuchi M *et al.* Cas12a *trans*-cleavage can be modulated *in vitro* and is active on ssDNA, dsDNA, and RNA. bioRxiv, https://doi.org/10.1101/600890, 08 April 2019, preprint: not peer reviewed.
4. Li S-Y, Cheng Q-X, Liu J-K *et al.* CRISPR-Cas12a has both *cis*- and *trans*-cleavage activities on single-stranded DNA. *Cell Res* 2018;28:491–3. https://doi.org/10.1038/s41422-018-0022-x
5. Zetsche B, Gootenberg JS, Abudayyeh OO *et al.* Cpf1 Is a single RNA-guided endonuclease of a class 2 CRISPR-Cas system. *Cell* 2015;163:759–71. https://doi.org/10.1016/j.cell.2015.09.038
6. Yang R, Zhao L, Wang X *et al.* Recent progress in aptamer and CRISPR-Cas12a based systems for non-nucleic target detection. *Crit Rev Anal Chem* 2023;0:1–18.
7. Yamano T, Nishimasu H, Zetsche B *et al.* Crystal structure of Cpf1 in complex with guide RNA and target DNA. *Cell* 2016;165:949–62. https://doi.org/10.1016/j.cell.2016.04.003
8. Swarts DC, van der Oost J, Jinek M. Structural basis for guide RNA processing and seed-dependent DNA targeting and cleavage by CRISPR-Cas12a. *Mol Cell* 2017;66:221–33. https://doi.org/10.1016/j.molcel.2017.03.016
9. Strohkendl I, Saha A, Moy C *et al.* Cas12a domain flexibility guides R-loop formation and forces RuvC resetting. *Mol Cell* 2024;84:2717–31. https://doi.org/10.1016/j.molcel.2024.06.007
10. Wörle E, Newman A, D'Silva J *et al.* Allosteric activation of CRISPR-Cas12a requires the concerted movement of the bridge helix and helix 1 of the RuvC II domain. *Nucleic Acids Res* 2022;50:10153–68.
11. Swarts DC, Jinek M. Mechanistic insights into the *cis*- and *trans*-acting DNase activities of Cas12a. *Mol Cell* 2019;73:589–600. https://doi.org/10.1016/j.molcel.2018.11.021
12. Newman A, Saha A, Starrs L *et al.* CRISPR-Cas12a REC2–Nuc interactions drive target-strand cleavage and constrain *trans* cleavage. *Nucleic Acids Res* 2025;53:gkaf988. https://doi.org/10.1093/nar/gkaf988

Downloaded from https://academic.oup.com/nar/article/54/1/gkaf1485/8418215 by guest on 26 March 2026

13. Strohkendl I, Saifuddin FA, Rybarski JR *et al.* Kinetic basis for DNA target specificity of CRISPR-Cas12a. *Mol Cell* 2018;71:816–24. https://doi.org/10.1016/j.molcel.2018.06.043
14. Naqvi MM, Lee L, Montaguth OET *et al.* CRISPR–Cas12a-mediated DNA clamping triggers target-strand cleavage. *Nat Chem Biol* 2022;18:1014–22. https://doi.org/10.1038/s41589-022-01082-8
15. van Aelst K, Martínez-Santiago CJ, Cross SJ *et al.* The effect of DNA topology on observed rates of R-loop formation and DNA strand cleavage by CRISPR Cas12a. *Genes* 2019;10:169. https://doi.org/10.3390/genes10020169
16. Pan J, Mabuchi M, Kneller DW *et al.* Kinetic analysis and engineering of thermostable Cas12a for nucleic acid detection. *Nucleic Acids Res* 2025;53:gkaf509. https://doi.org/10.1093/nar/gkaf509
17. Yamano T, Zetsche B, Ishitani R *et al.* Structural basis for the canonical and non-canonical PAM recognition by CRISPR-Cpf1. *Mol Cell* 2017;67:633–45. https://doi.org/10.1016/j.molcel.2017.06.035
18. Saha A, Ahsan M, Arantes PR *et al.* An alpha-helical lid guides the target DNA toward catalysis in CRISPR-Cas12a. *Nat Commun* 2024;15:1473. https://doi.org/10.1038/s41467-024-45762-6
19. Nalefski EA, Patel N, Leung PJY *et al.* Kinetic analysis of Cas12a and Cas13a RNA-guided nucleases for development of improved CRISPR-based diagnostics. *iScience* 2021;24:102996. https://doi.org/10.1016/j.isci.2021.102996
20. Nalefski EA, Hedley S, Rajaraman K *et al.* Unleashing high trans-substrate cleavage kinetics of Cas12a for nucleic acid diagnostics. *Nucleic Acids Res* 2025;53:gkaf712. https://doi.org/10.1093/nar/gkaf712
21. Varadi M, Anyango S, Deshpande M *et al.* AlphaFold Protein Structure Database: massively expanding the structural coverage of protein-sequence space with high-accuracy models. *Nucleic Acids Res* 2022;50:D439–44. https://doi.org/10.1093/nar/gkab1061
22. Meng EC, Goddard TD, Pettersen EF *et al.* UCSF ChimeraX: tools for structure building and analysis. *Protein Sci* 2023;32:e4792. https://doi.org/10.1002/pro.4792
23. Oppenheim A. Separation of closed circular DNA from linear DNA by electrophoresis in two dimensions in agarose gels. *Nucleic Acids Res* 1981;9:6805–12. https://doi.org/10.1093/nar/9.24.6805
24. Rueden CT, Schindelin J, Hiner MC *et al.* ImageJ2: imageJ for the next generation of scientific image data. *BMC Bioinformatics* 2017;18:529. https://doi.org/10.1186/s12859-017-1934-z
25. Cofsky JC, Karandur D, Huang CJ *et al.* CRISPR-Cas12a exploits R-loop asymmetry to form double-strand breaks. *eLife* 2020;9:e55143. https://doi.org/10.7554/eLife.55143
26. Stella S, Mesa P, Thomsen J *et al.* Conformational activation promotes CRISPR-Cas12a catalysis and resetting of the endonuclease activity. *Cell* 2018;175:1856–71. https://doi.org/10.1016/j.cell.2018.10.045
27. Kleinstiver BP, Sousa AA, Walton RT *et al.* Engineered CRISPR–Cas12a variants with increased activities and improved targeting ranges for gene, epigenetic and base editing. *Nat Biotechnol* 2019;37:276–82. https://doi.org/10.1038/s41587-018-0011-0
28. Zhang L, Zuris JA, Viswanathan R *et al.* AsCas12a ultra nuclease facilitates the rapid generation of therapeutic cell medicines. *Nat Commun* 2021;12:3908. https://doi.org/10.1038/s41467-021-24017-8
29. Rossetti M, Merlo R, Bagheri N *et al.* Enhancement of CRISPR/Cas12a *trans*-cleavage activity using hairpin DNA reporters. *Nucleic Acids Res* 2022;50:8377–91. https://doi.org/10.1093/nar/gkac578
30. Lv H, Wang J, Zhang J *et al.* Definition of CRISPR Cas12a *trans*-cleavage units to facilitate CRISPR diagnostics. *Front Microbiol* 2021;12:766464. https://doi.org/10.3389/fmicb.2021.766464
31. Rananaware SR, Vesco EK, Shoemaker GM *et al.* Programmable RNA detection with CRISPR–Cas12a. *Nat Commun* 2023;14:5409. https://doi.org/10.1038/s41467-023-41006-1
32. Thaplyal P, Bevilacqua PC. Experimental approaches for measuring pKa's in RNA and DNA. *Methods Enzymol* 2014;549:189–219.
33. Overman LB, Lohman TM. Linkage of pH, anion and cation effects in protein-nucleic acid equilibria: *Escherichia coli* SSB protein-single stranded nucleic acid interactions. *J Mol Biol* 1994;236:165–78. https://doi.org/10.1006/jmbi.1994.1126
34. Guo LY, Bian J, Davis AE *et al.* Multiplexed genome regulation *in vivo* with hyper-efficient Cas12a. *Nat Cell Biol* 2022;24:590–600. https://doi.org/10.1038/s41556-022-00870-7
35. Hildes J, Ferguson M. The concentration of electrolytes in normal human saliva. *Can J Biochem Physiol* 1955;33:217–25. https://doi.org/10.1139/y55-031
36. Wei Y, Zhou Y, Liu Y *et al.* Indiscriminate ssDNA cleavage activity of CRISPR–Cas12a induces no detectable off-target effects in mouse embryos. *Protein Cell* 2021;12:741–5. https://doi.org/10.1007/s13238-021-00824-z
37. Marino ND, Pinilla-Redondo R, Bondy-Denomy J. CRISPR–Cas12a targeting of ssDNA plays no detectable role in immunity. *Nucleic Acids Res* 2022;50:6414–22. https://doi.org/10.1093/nar/gkac462
38. Liu S, Rao X, Zhao R *et al.* The *trans* DNA cleavage activity of Cas12a provides no detectable immunity against plasmid or phage. *Front Genome Ed* 2022;4: 929929. https://doi.org/10.3389/fgeed.2022.929929
39. Ashton NW, Bolderson E, Cubeddu L *et al.* Human single-stranded DNA binding proteins are essential for maintaining genomic stability. *BMC Mol Biol* 2013;14:9. https://doi.org/10.1186/1471-2199-14-9
40. Liu B, Poolman B, Boersma AJ. Ionic strength sensing in living cells. *ACS Chem Biol* 2017;12:2510–4. https://doi.org/10.1021/acschembio.7b00348
41. Romani AMP. Cellular magnesium homeostasis. *Arch Biochem Biophys* 2011;512:1–23. https://doi.org/10.1016/j.abb.2011.05.010
42. Nguyen LT, Macaluso NC, Rakestraw NR *et al.* Harnessing noncanonical crRNAs to improve functionality of Cas12a orthologs. *Cell Rep*;2024;43:113777. https://doi.org/10.1016/j.celrep.2024.113777
43. Fuchs RT, Curcuru JL, Mabuchi M *et al.* Characterization of Cme and Yme thermostable Cas12a orthologs. *Commun Biol* 2022;5:1–16. https://doi.org/10.1038/s42003-022-03275-2
44. Youngquist BM, Saliba J, Kim Y *et al.* Rapid tuberculosis diagnosis from respiratory or blood samples by a low cost, portable lab-in-tube assay. *Sci Transl Med* 2025;17:eadp6411. https://doi.org/10.1126/scitranslmed.adp6411
45. Nalefski EA, Sinan S, Cantera JL *et al.* Room temperature CRISPR diagnostics for low-resource settings. *Sci Rep* 2025;15:3909. https://doi.org/10.1038/s41598-025-86373-5
46. Singh D, Mallon J, Poddar A *et al.* Real-time observation of DNA target interrogation and product release by the RNA-guided endonuclease CRISPR Cpf1 (Cas12a). *Proc Natl Acad Sci USA* 2018;115:5444–9. https://doi.org/10.1073/pnas.1718686115

Downloaded from https://academic.oup.com/nar/article/54/1/gkaf1485/8418215 by guest on 26 March 2026

Received: November 10, 2025. **Revised:** December 7, 2025. **Accepted:** December 11, 2025
© The Author(s) 2026. Published by Oxford University Press.
This is an Open Access article distributed under the terms of the Creative Commons Attribution License (https://creativecommons.org/licenses/by/4.0/), which permits unrestricted reuse, distribution, and reproduction in any medium, provided the original work is properly cited.